

# Carbon Nanotube Microarchitectures for Enhanced Thermal Conduction at Ultralow Mass Fraction in Polymer Composites

By Michael Bozlar, Delong He, Jinbo Bai, Yann Chalopin, Natalio Mingo, and Sebastian Volz\*

Among a broad range of carbonaceous materials, such as exfoliated graphite,<sup>[1]</sup> graphene or diamond, carbon nanotubes (CNTs) are widely used as a thermal filler because of their exceptional intrinsic thermal conductivity (TC) and aspect ratios, which are larger than 1000. The TC of single-walled CNTs (SWNTs) has been reported<sup>[2]</sup> as high as  $6000 \text{ W m}^{-1} \text{ K}^{-1}$ , and that of multi-walled CNTs (MWNTs) was experimentally measured at  $3075 \text{ W m}^{-1} \text{ K}^{-1}$  at room temperature,<sup>[3]</sup> which remains above the performances of diamond ( $\text{TC} = 2200 \text{ W m}^{-1} \text{ K}^{-1}$ ).<sup>[4,5]</sup> Therefore the improvement of the TC of composites based on CNTs was extensively investigated over the past years.<sup>[6,7]</sup> A recent work revealed that a TC of  $0.28 \text{ W m}^{-1} \text{ K}^{-1}$  or a 40% increase had been reached in composites with a 10% weight fraction (wt%) of CNTs dispersed in polyvinylacetate matrix by using the classical sonication method.<sup>[8]</sup> Another optimized configuration was proposed by Haddon and co-workers, who brought into play a hybrid filler based on the combination of SWNTs and graphite nanoplatelets.<sup>[9]</sup> An improved TC of  $1.7 \text{ W m}^{-1} \text{ K}^{-1}$ —about a fivefold increase—was obtained for epoxy composites. The hybrid loading mass fraction was as high as 10%, including 7 wt% graphite nanoplatelets and 3 wt% SWNTs.

Those wt% appear to be far larger than the one of percolation, which should be smaller than 0.1% in CNT-reinforced composites.<sup>[10]</sup> The percolation should yield a significant TC augmentation that has not yet been observed. A previous investigation on CNT-based nanofluids emphasized that the TC of the mixture remains thirty times lower than the expected theoretical value and much worse at low mass fractions.<sup>[11]</sup> This unsatisfying behavior was attributed to interfacial contact resistances,<sup>[12]</sup> which several teams tried to reduce, but with little success. We have also evaluated the TC of CNT pellets in vacuum from the number of thermal contacts between CNTs, and obtained stringent theoretical limitations that are confirmed by experiment.<sup>[13]</sup> It is very plausible that the TC improvement at percolation was never achieved in practice due to insufficient CNT dispersion leading to the predominance of thermal contact resistances.<sup>[11]</sup> In many cases indeed, no efficient percolating networks are visible.<sup>[8]</sup>

In this communication, we demonstrate that epoxy composites with extremely low CNT wt% corresponding to the percolation can have the predicted TC values, which are as high as those previously obtained at a wt% one order of magnitude larger.

This new field of properties can indeed be reached by a microarchitecture involving  $\text{Al}_2\text{O}_3$  microparticles and MWNTs. These multiscale fillers belong to a new generation of hybrid materials, where alumina microparticles provide efficient structures by dispersing the CNT network within the polymer matrix. To further improve the dispersion, we have also implemented mechanical dispersion of the  $\text{Al}_2\text{O}_3$ -CNTs hybrid fillers without any chemical pretreatment. The result is a drastic decrease in the number of thermal contacts between the CNTs. As a consequence, our modeling reveals that the TC of the obtained material does not depend on the contact resistances between CNTs, but only on the CNTs thermal conductivity and geometry. Indeed, the percolation is generated and the predicted TC enhancement of 130% at CNT mass fractions of only 0.15%, ten times lower than previous state-of-the-art research, is measured.

Two types of fillers (CNTs and  $\text{Al}_2\text{O}_3$ -CNTs) are prepared using chemical vapor deposition<sup>[14]</sup> (CVD) synthesis, as described in our previous work.<sup>[15,16]</sup> Pristine MWNTs are formed in bundles with a density of  $1.87 \text{ g cm}^{-3}$  and the well-structured hybrid fillers are obtained by growing in-situ MWNTs that are homogeneously self-organized on the surface of micrometric ceramic particles (Fig. 1). The spherical particles are present in the  $\alpha$ -alumina (hexagonal) crystal phase with an average diameter  $D$  ranging

[\*] Dr. S. Volz, Y. Chalopin

Laboratoire d'Énergétique Moléculaire, Macroscopique et Combustion  
Ecole Centrale Paris, CNRS UPR288, PRES UniverSud Paris  
Grande Voie des Vignes, 92295 Châtenay-Malabry Cedex (France)  
E-mail: volz@iis.u-tokyo.ac.jp

Dr. S. Volz

Laboratory for Integrated Micro-Mechatronic Systems  
Institute of Industrial Science, University of Tokyo, CNRS UMI2820  
4-6-1 Komaba, Meguro-ku, Tokyo 153-8505 (Japan)

M. Bozlar, Dr. J. Bai, D. He

Laboratoire de Mécanique des Sols, Structures et Matériaux  
Ecole Centrale Paris, CNRS UMR8579, PRES UniverSud Paris  
Grande Voie des Vignes, 92295 Châtenay-Malabry Cedex (France)

M. Bozlar

Laboratoire de Photophysique, Photochimie, Supramoléculaires et  
Macromoléculaires  
Ecole Normale Supérieure de Cachan, CNRS UMR8531, PRES  
UniverSud Paris  
61 Avenue du Président Wilson, 94235 Cachan Cedex (France)

Dr. N. Mingo

LITEN, CEA-Grenoble  
17 rue des Martyrs, 38054 Grenoble Cedex (France)

DOI: 10.1002/adma.200901955

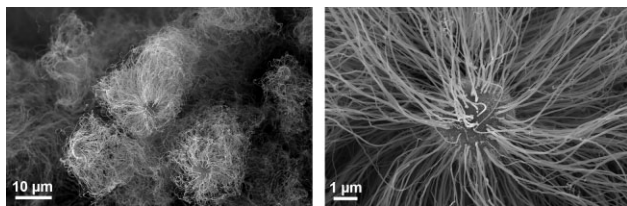


**Figure 1.** SEM images of Al<sub>2</sub>O<sub>3</sub>-CNT hybrids. Homogeneously structured micro-nanometric hybrids are obtained by CVD. The overall diameter of the Al<sub>2</sub>O<sub>3</sub>-CNT hybrid filler is  $\approx 30 \mu\text{m}$ ; the average length and diameter of the MWNTs are  $13 \mu\text{m}$  and  $40 \text{nm}$ , respectively. Thermogravimetric analyses indicate that the average wt% of CNTs on one alumina particle is 20%.

from 2 to  $7 \mu\text{m}$  and a density of  $3.69 \text{g cm}^{-3}$ . Further Raman spectroscopy was performed on the two types of fillers and pristine  $\alpha\text{-Al}_2\text{O}_3$  (see Supporting Information, Fig. S1). Specific peaks corresponding to alumina and CNTs were identified in conformity with previous studies.<sup>[17,18]</sup> The two fillers have similar structures, and  $\alpha\text{-Al}_2\text{O}_3$  does not favor the formation of defects in CNTs.

Diglycidyl ether of bisphenol A (DGEBA), commonly known as epoxy, serves as the matrix in the nanocomposites. Among the methods cited in the literature for dispersing micrometric or nanometric fillers,<sup>[19,20]</sup> chemical surface functionalization is widely used.<sup>[16,21,22]</sup> Nevertheless, hard chemical modifications using surfactants can deteriorate the electrical and thermal properties of CNTs. Therefore, an alternative method involving mechanical strain is implemented in this work. A three-roll mill allows for applying controlled pressure and shear forces on the fluid containing the mixture of CNTs and epoxy resin.<sup>[23]</sup> By controlling the gap between the rolls, their rotation speed, and the residence time of the liquid in the machine, we have finally optimized the dispersion of the fillers, as displayed in Figure 2. Naturally, the viscosity of the blend decreased due to the mechanical forces applied on it. It has thus been deduced that the nanofiller organization is strongly related to the blending time and the gap between the rolls. Note that a too long blending time generates the detachment of CNTs from the surface of ceramic particles leading to the nanofillers aggregating again.

TC characterizations were carried out on nanocomposites (1 mm thick,  $10 \text{mm} \times 10 \text{mm}$  cross-section) with a noncontact method thanks to a light flash apparatus LFA 447<sup>[12,24]</sup> at  $20^\circ\text{C}$ . Differential scanning calorimetry (DSC) analyses were performed

to estimate the sample's specific heat  $C_p$  at  $20^\circ\text{C}$  (see Supporting Information, Table 1 and 2). The average bulk densities  $\rho$  for the epoxy/CNTs and epoxy/Al<sub>2</sub>O<sub>3</sub>-CNTs nanocomposites were measured at  $1.10$  and  $1.13 \text{g cm}^{-3}$ , respectively. Finally, the  $\kappa$  of TC is calculated from the relation:

$$\kappa = \rho C_p \alpha \quad (1)$$

where  $\alpha$  is the thermal diffusivity. The room temperature TCs of epoxy polymer and  $\alpha$ -alumina particles of  $\kappa_m = 0.17 \text{W m}^{-1} \text{K}^{-1}$  and  $\kappa_{\text{Al}_2\text{O}_3} = 46 \text{W m}^{-1} \text{K}^{-1}$  respectively, are obtained from the literature and confirmed by our experiments.<sup>[19,25]</sup> The prediction of  $\kappa$  is conducted in a preliminary stage by deriving the nonpercolating Al<sub>2</sub>O<sub>3</sub>-CNT hybrid fillers. The approximations of a small volume fraction  $\eta$  of the filler ( $< 0.3\%$ ) and a large filler TC compared to the one of the matrix yield:<sup>[26]</sup>

$$\kappa = \kappa_m (1 + 3\eta) \quad (2)$$

Note that the contact resistance between the filler and the matrix is neglected, which is a reasonable guess due to the very low TC of the epoxy. Equation 2 clearly shows i) that the TC contribution of the hybrid fillers is added to that of the matrix, which supports the idea that the filler contribution is not correlated to that of the matrix and ii) that this TC contribution in relative value should not exceed the wt% because  $3\eta \approx \eta \rho_{\text{Al}_2\text{O}_3} / \rho_{\text{Epoxy}} = < 1 \text{wt}\%$ . The increase in TC obtained when adding CNTs is larger than 100% instead. The result of Equation 2 therefore leads to the conclusion that only percolating CNTs are responsible for this outstanding augmentation. Another consequence of Equation 2 is that the effect of the heat conduction of the alumina microparticles, if taken as the only filler, is remarkably negligible. This point supports the assertion that the only role of the microparticles is to structure the CNTs with optimal dispersion in such a way that it seems sound to compare the TCs of hybrid charges and pure CNT-based samples according to their CNT wt%.

First, this model quantifies the TC of the nanocomposites for a specified microparticle diameter  $D$  by establishing a simple model based on a cubic element of edge length  $L$ , which includes one microparticle and its surrounding CNTs, as illustrated in Figure 3a. We express the thermal resistance in one direction in

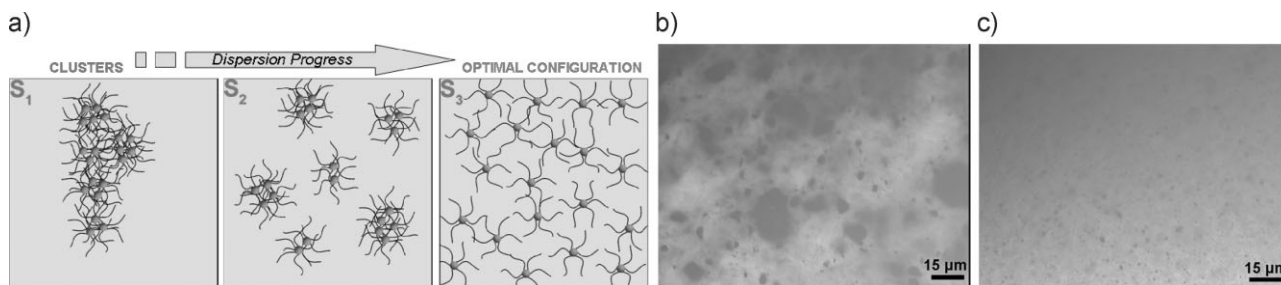


**Figure 2.** Fillers dispersion in epoxy. a) The schematic represents the spatial arrangements of Al<sub>2</sub>O<sub>3</sub>-CNT fillers within a polymer. Fillers dispersion is chronologically represented from the state S<sub>1</sub> (beginning of the dispersion process) to S<sub>3</sub> (end). b,c) Optical microscope images indicate pristine CNT dispersion in the monomer obtained by using a contrast-enhanced silicon wafer after 5 (b: heterogeneous dark areas) and 20 min (c: homogeneous medium).

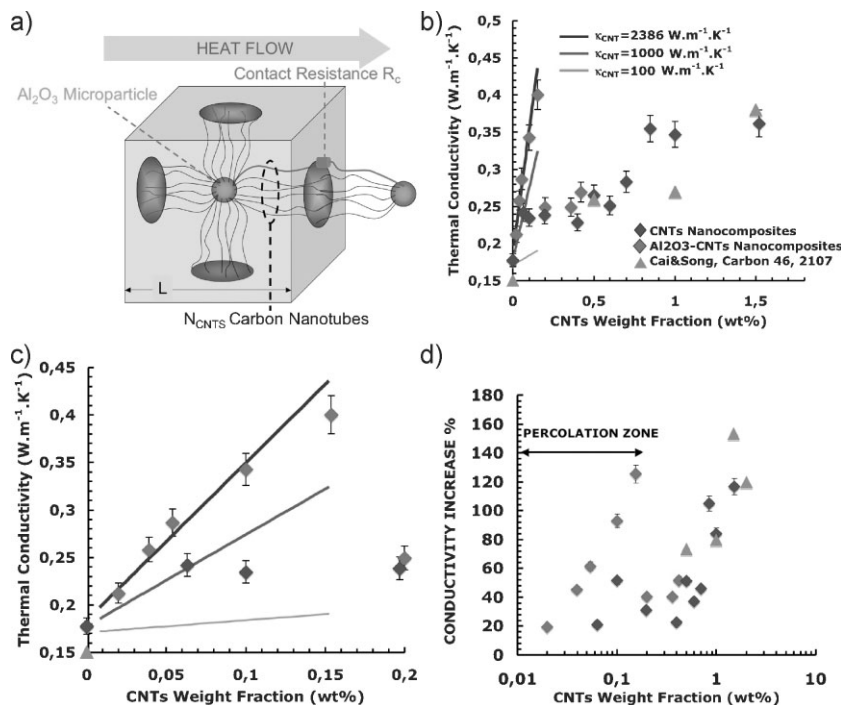


**Figure 3.** a) Schematic of the cubic element used in the model yielding the hybrid filler TC. b–d) Nanocomposites TCs versus CNT wt%. In schematic (a), the thermal resistance of the cube is modeled in the direction of the heat flow.  $R_C$  is the thermal contact resistance between two CNTs linking two microparticles belonging to two neighboring cubes.  $N_{CNTs}$  is the number of those CNTs having the length  $L_{CNT}$ , the cross-section  $S_{CNT}$  and the TC  $\kappa_{CNT}$ . Note that CNTs with directions perpendicular to the cube front face are not represented. b–d) The measured TCs of the hybrid  $Al_2O_3$  microparticles–CNT fillers (red diamonds) and of the CNT-based composites (blue diamonds) described in this work are reported as well as recent data from the literature [27] (grey triangles). The prediction of Equation 6 is also indicated for the TC of the CNTs:  $2386 \text{ W m}^{-1} \text{ K}^{-1}$  (dark green thick line),  $1000 \text{ W m}^{-1} \text{ K}^{-1}$  (green line), and  $100 \text{ W m}^{-1} \text{ K}^{-1}$  (light green thin line). The TC enhancement at ultralow mass fraction of hybrid fillers is clearly identified (c). The epoxy TC increases as a function of the CNTs wt% (d). The one order of magnitude difference in wt% between the hybrid  $Al_2O_3$ –CNTs and pristine CNTs TC augmentation is clearly emphasized.

this volume at the percolation threshold. This resistance is decomposed into the microparticle resistance, the thermal resistances of the CNTs having approximately the same direction as the heat flow, and the contact resistance between the CNTs linking two microparticles. It can be easily shown that the microparticle resistance is significantly smaller than that of the CNTs and that of the CNT–CNT contacts. Consequently, the filler TC  $\kappa_F$  arises from the Fourier law of heat conduction as a function of the CNT length  $L_{CNT}$ , cross-section  $S_{CNT}$ , and TC  $\kappa_{CNT}$  as well as of the number  $N_{CNTs}$  of CNTs linking two microparticles in the following form:

$$\kappa_F = N_{CNTs} \left[ \frac{2L_{CNT}}{\kappa_{CNT} S_{CNT}} + R_C \right]^{-1} / L = N_{CNTs} \frac{G_{CNT}}{L} \quad (3)$$

The term inside brackets can be identified as the conductance  $G_{CNT}$  associated with two CNTs in contact.  $R_C$ , which represents the contact resistance between two CNTs due to weak Van der Waals interactions, can be derived from Reference [13] by rescaling the published data obtained for small CNT diameters by

the ratio of the CNT cross-sections—the resistance  $R_C$  being reversely proportional to the contact area and the ratio of the contact areas being equal to the ratio of the cross-sections—which provides the value of  $R_C = 9.26 \times 10^6 \text{ K W}^{-1}$ .  $\kappa_{CNT}$  is extracted from Reference [3] owing to a linear interpolation depending on the CNT diameter. The obtained value of  $\kappa_{CNT} = 2386 \text{ W m}^{-1} \text{ K}^{-1}$  is kept as a reference. The total number of CNTs noted  $N$  on one microparticle can be deduced from the known ratio of 0.25 between the mass of the  $N$  and the mass of one microparticle. We assume a homogenous percolation where the microparticles form a cubic lattice in such a way that  $N_{CNTs} = N/6$  CNTs are linked with another microparticle because of the six possible directions available in a cubic lattice. The second neighbors are not percolating and are consequently excluded.

The ratio between the contact resistance  $R_C$  and CNTs resistances  $2L_{CNT}/\kappa_{CNT} S_{CNT}$  being in the order of 0.516, we infer that the contributions of the contact resistance and the CNTs resistances are in competition. A noticeable predominance of CNTs resistance can still be established.

In a second phase, the distribution of the microparticle diameter, which is supposed to be uniform, is taken into account. The values of  $N_{CNTs}$  and  $L = 2L_{CNT} + D$  at a given microparticle diameter  $D$  are indeed imposed by the homogenous percolation or the equality between  $L$  and the lattice constant of a cubic lattice formed by the microparticles. This equality yields the following mass fraction at percolation:

$$wt = 0.13 \frac{\rho_{Al_2O_3}}{\rho_{Epoxy}} \left( \frac{D}{L} \right)^3 \quad (4)$$

This simplified expression is obtained by noticing that the CNT mass in the cubic element equals the mass of one microparticle divided by four. Considering  $D$  in the range of 2–7  $\mu\text{m}$ , the corresponding mass fraction is found in the interval of 0.01–0.3%. Introducing the mass fraction in Equation 3 brings the following new expression for the TC:

$$\kappa(wt) - \kappa_m = wt \frac{m_{Epoxy}}{6m_{CNT}} \frac{G_{CNT}}{L} \quad (5)$$

where  $m_{CNT}$  and  $m_{Epoxy}$  are the masses of one CNT and of the epoxy included in the  $L^3$  volume, respectively. Starting from the lowest mass fraction where only the smallest microparticles will percolate, we progressively add the contributions of larger microparticles as wt% increases by integrating and normalizing the second term in the right-hand side (RHS) of Equation 5

between the lowest and the running mass fractions,  $wt_{\min}\%$  calculated from Equation 4 when  $D=2\ \mu\text{m}$  and  $wt\%$ , respectively, in order to reach the following expression:

$$\kappa_{\text{tot}}(wt) - \kappa_m = \frac{wt + wt_{\min}}{2} \frac{m_{\text{Epoxy}}}{6m_{\text{CNT}}} \frac{G_{\text{CNT}}}{L} \quad (6)$$

The TC increase appears as proportional to the  $wt\%$  as well as to  $\kappa_{\text{CNT}}$  and  $S_{\text{CNT}}$  and reversely proportional to  $L$  and  $L_{\text{CNT}}$ . The validity of this cumulative description relies on the assumption that the percolating networks based on microparticles with different diameters do not interfere. The TC measurements for nanocomposites filled with hybrids and CNTs are reported in Figure 3b–d versus the CNT  $wt\%$ , together with those of the literature<sup>[27]</sup> when the CNTs are chemically treated with sodium dodecyl sulfate (SDS) surfactant.

The agreement between our model and experimental values appears when  $\kappa_{\text{CNT}}$  approaches the reference value of  $2386\ \text{W m}^{-1}\ \text{K}^{-1}$ , an optimal match between the model and the first four points is reached when  $\kappa_{\text{CNT}}=2180\ \text{W m}^{-1}\ \text{K}^{-1}$ , which proves that the TC of the single CNT is retrieved within an inaccuracy range smaller than 10% in the composite, and that the theoretical percolation limit is also obtained. In Figure 3b–d, the TC of the hybrid-filler-based composite increases rapidly at  $wt\%$  starting from 0.02 to 0.15% and reaches the value of  $0.4\ \text{W m}^{-1}\ \text{K}^{-1}$ , which is 130% more than the epoxy TC. To our knowledge, none of the previous work proposing CNT-based nanocomposites could succeed in preserving the unique thermal property of one MWNT when including it as filler in a polymer composite. This increase also proves that the early percolation due to the high aspect ratio of CNTs is adequately generated starting with the smaller microparticles and then involving larger ones. When comparing the TCs of hybrid filler composite materials to those of CNTs based samples, the curves in Figure 3 reveal that the same TC increase appears, but at a  $wt\%$  smaller by one order of magnitude. Comparison with previous experimental data in the literature<sup>[19,23,27]</sup> tends to emphasize that our mechanical dispersion process seems to be superior to those based on chemical treatment<sup>[27]</sup> (e.g., SDS surfactant) of CNTs, because the TC of our CNTs without any pretreatment increases at lower  $wt\%$ . This outcome is supported by previous works showing that CNT dispersion in a thermoplastic polymer is efficiently achieved under mechanical strains.<sup>[28]</sup>

After the extraordinary increase of the TC for  $wt\%$  up to 0.15%, the TC of the hybrid-filler-based sample drastically decreases to the level of the CNT composites. The first explanation is that the CNT surface becomes so large that the liquid matrix cannot fill all the interstices in such a way that air bubbles with a very low TC remain in the composite. DSC analyses confirm that at high filler loadings, the structure of the polymer matrix is altered, which leads to the disruption of the nanotube–polymer interface, and also to interphase creation.<sup>[29]</sup> This change in behavior is indicated by the modification of the glass transition temperature  $T_g$  located at  $70\ ^\circ\text{C}$  at low mass fractions, but reaching higher values  $\approx 100\ ^\circ\text{C}$  for loadings larger than 0.15%. Such increase of the  $T_g$  attests the earlier arrest of the molecular chain dynamics. During composite preparation, the viscosity of the blend strongly increases for CNT mass fractions larger than 0.15%, in such a way

that the mixing between epoxy and hybrid fillers becomes more difficult to achieve. Ultimately, when nanocomposites have high filler loadings, only a few air bubbles are visible during scanning electron microscopy (SEM) analyses (see Supporting Information, Fig. S2). The second explanation is that the area occupied by the CNTs on the microparticle increases more rapidly than the microparticle surface as the  $wt\%$  increases. Our fabrication process implies that the ratio between both surfaces is indeed proportional to  $(wt\%)^{1/3}$ . When the CNT density on the microparticle surface becomes too high, CNTs agglomerate and form only a few very wide bundles in such a way that the percolation is broken (see Supporting Information, Fig. S3). The last reason for the TC diminution at  $w\%=0.15\%$  is the increase of the number of contacts between CNTs when the mass fraction exceeds the one of percolation.

Additional fabrication and characterization of epoxy– $\text{Al}_2\text{O}_3$  nanocomposites loaded at 0.5 and 1  $wt\%$  have provided TCs of 0.23 and  $0.16\ \text{W m}^{-1}\ \text{K}^{-1}$ , respectively. Those figures highlight the degradation of the thermal performances after reaching a  $wt\%$  of 1% even without the presence of CNTs. This result tends to corroborate the evolution of the TC in our  $\text{Al}_2\text{O}_3$ –CNT polymer composites. These explanations might open the path for new improvements, but we emphasize that using CNTs at mass fractions larger than that of percolation does not take advantage of the CNT assets that are put forward in this work.

In summary, we report in this communication on the remarkably low percolation threshold and high TC of  $\text{Al}_2\text{O}_3$ –CNT-filler-based nanocomposites taking advantage of the large aspect ratio of CNTs as well as of their unique TC. Preserving the TC of one MWNT and observing the theoretical percolation from the TC evolution is proven for the first time in this work. This new field of performances is unlocked by generating a CNT microarchitecture as well as by developing a mechanical dispersion. We believe that this structuration and dispersion have significantly reduced the number of thermal contact resistances between the CNTs. The result is an excellent CNT dispersion leading to the observed limit properties. We expect a very significant impact for thermal interface materials especially concerning microelectronic devices through the increase of the TC of packaging material. The design of an industrial composite material combining improved thermal performances and satisfying mechanical properties that are not affected by a high filler loading, also becomes achievable.

## Experimental

**Filler and Composite Preparation:** The as received  $\alpha$ -alumina powder (Sumitomo Chemical Co. Ltd, Japan) with a purity of 99.8% was scattered on the surface of a  $\text{SiO}_2$  substrate. In a second step, a mixture of xylene,  $\text{C}_8\text{H}_{10}$ , and ferrocene,  $\text{Fe}(\text{C}_5\text{H}_5)_2$ , with a concentration of  $(0.05\ \text{g mL}^{-1})$  was injected into a reactor at  $750\ ^\circ\text{C}$ , over a period of 10 min, for the CNT growth. A solution comprising fillers and monomer was dispersed thanks to a three-roll mill (Exakt Vertriebs GmbH, Germany) following a well-established protocol. Then, an appropriate amount of hardener at the relevant stoichiometry was added to the latter solution. Afterwards it was cast into an aluminum mould (designed in our laboratory in agreement with ISO 527 and ASTM D638 standards) and followed by successive vacuum in order to remove air bubbles. Samples were cured at room temperature for 12 h. Finally, a postcure at  $90\ ^\circ\text{C}$  for 6 h was performed to ensure complete of curing.

**Thermal Analyses:** The thermal diffusivity  $\alpha$  was measured by using the following methodology: first, the front side of the sample was heated by a short Xenon light impulse while an infrared detector measured the resulting temperature rise on the back surface versus time. Secondly, the detector signal was analyzed with the 1D transient heat conduction equation yielding the value of  $\alpha$  within 5% of accuracy. The measurements were repeated 3 times and excellent reproducibility of the experiments was concluded. DSC analyses were performed on nanocomposites (weights between 5–8 mg) with a Diamond DSC Perkin Elmer. To confirm curing, a first cycle from 30 to 260 °C by a 10 °C min<sup>-1</sup> temperature ramp, and then cooling at 5 °C min<sup>-1</sup> back to 30 °C was realized.  $T_g$  and  $C_p$  were acquired on a second cycle from 0 to 200 °C (heating) and then cooling to 30 °C.

**SEM Characterizations:** Field-emission SEM observations were realized using a LEO Gemini 1530 operated at 5 kV. Nanocomposites were broken in liquid nitrogen and the fractured surface was metalized with tungsten using a Gatan 682 coating system.

**Spectroscopy:** Raman spectroscopy was performed using a microspectrometer Renishaw Raman RM, (resolution: 1 cm<sup>-1</sup>) at room temperature. Spectra were acquired with the 514.5 nm line from an Argon ion laser for excitation.

## Acknowledgements

Michael Bozlar is thankful to collaborators from ENS Cachan: Arnaud Brosseau, for his technical assistance with DSC measurements, Prof. Fabien Miomandre and Prof. Pierre Audebert for precious advice. Supporting Information is available online from Wiley InterScience or from the author.

Received: June 10, 2009

Revised: August 25, 2009

Published online: December 8, 2009

- [1] L. M. Veca, M. J. Meziani, W. Wang, X. Wang, F. Lu, P. Zhang, Y. Lin, R. Fee, J. W. Connell, Y. P. Sun, *Adv. Mater.* **2009**, *21*, 2088.
- [2] S. Berber, Y. K. Kwon, D. Tomanek, *Phys. Rev. Lett.* **2000**, *84*, 4613.
- [3] P. Kim, L. Shi, A. Majumdar, P. L. McEuen, *Phys. Rev. Lett.* **2001**, *87*, 4.
- [4] T. H. Kim, W. M. Choi, D. H. Kim, M. A. Meitl, E. Menard, H. Q. Jiang, J. A. Carlisle, J. A. Rogers, *Adv. Mater.* **2008**, *20*, 2171.
- [5] J. E. Graebner, S. Jin, G. W. Kammlott, J. A. Herb, C. F. Gardinier, *Nature* **1992**, *359*, 401.
- [6] H. M. Duong, D. V. Papavassiliou, K. J. Mullen, S. Maruyama, *Nanotechnology* **2008**, *19*, 8.
- [7] H. Huang, C. H. Liu, Y. Wu, S. S. Fan, *Adv. Mater.* **2005**, *17*, 1652.
- [8] C. Yu, Y. S. Kim, D. Kim, J. C. Grunlan, *Nano Lett.* **2008**, *8*, 4428.
- [9] A. P. Yu, P. Ramesh, X. B. Sun, E. Bekyarova, M. E. Itkis, R. C. Haddon, *Adv. Mater.* **2008**, *20*, 4740.
- [10] M. Endo, M. S. Strano, P. M. Ajayan, in *Carbon Nanotubes*, Vol. 111 (Eds: A. Jorio, M. S. Dresselhaus, G. Dresselhaus) Springer, Berlin **2008**, p. 13.
- [11] S. T. Huxtable, D. G. Cahill, S. Shenogin, L. P. Xue, R. Ozisik, P. Barone, M. Usrey, M. S. Strano, G. Siddons, M. Shim, P. Keblinski, *Nat. Mater.* **2003**, *2*, 731.
- [12] W. Lin, K. S. Moon, C. P. Wong, *Adv. Mater.* **2009**, *21*, 2421.
- [13] a) R. S. Prasher, X. J. Hu, Y. Chalopin, N. Mingo, K. Lofgreen, S. Volz, F. Cleri, P. Keblinski, *Phys. Rev. Lett.* **2009**, *102*, 105901. b) Y. Chalopin, N. Mingo, S. Volz, *J. Appl. Phys.* **2009**, *105*, 84301.
- [14] Y. L. Li, I. A. Kinloch, A. H. Windle, *Science* **2004**, *304*, 276.
- [15] L. J. Ci, J. B. Bai, *Adv. Mater.* **2004**, *16*, 2021.
- [16] M. Bozlar, F. Miomandre, J. B. Bai, *Carbon* **2009**, *47*, 80.
- [17] A. M. Rao, P. C. Eklund, S. Bandow, A. Thess, R. E. Smalley, *Nature* **1997**, *388*, 257.
- [18] T. Azuhata, T. Sota, K. Suzuki, S. Nakamura, *J. Phys. Condens. Matter* **1995**, *7*, L129.
- [19] M. Moniruzzaman, K. I. Winey, *Macromolecules* **2006**, *39*, 5194.
- [20] P. M. Ajayan, J. M. Tour, *Nature* **2007**, *447*, 1066.
- [21] J. Zhu, J. D. Kim, H. Q. Peng, J. L. Margrave, V. N. Khabashesku, E. V. Barrera, *Nano Lett.* **2003**, *3*, 1107.
- [22] X. H. Peng, S. S. Wong, *Adv. Mater.* **2009**, *21*, 625.
- [23] E. T. Thostenson, T. W. Chou, *Carbon* **2006**, *44*, 3022.
- [24] S. Shaikh, L. Li, K. Lafdi, J. Huie, *Carbon* **2007**, *45*, 2608.
- [25] D. G. Cahill, S. M. Lee, T. I. Selinder, *J. Appl. Phys.* **1998**, *83*, 5783.
- [26] Y. Benveniste, *J. Appl. Phys.* **1987**, *61*, 2840.
- [27] D. Y. Cai, M. Song, *Carbon* **2008**, *46*, 2107.
- [28] S. B. Kharchenko, J. F. Douglas, J. Obrzut, E. A. Grulke, K. B. Migler, *Nat. Mater.* **2004**, *3*, 564.
- [29] K. W. Putz, M. J. Palmeri, R. B. Cohn, R. Andrews, L. C. Brinson, *Macromolecules* **2008**, *41*, 6752.